Orientation Dependence of Displacements by a Single One-Headed Myosin Relative to the Actin Filament

Hiroto Tanaka,* Akihiko Ishijima,#§ Makoto Honda*, Kiwamu Saito,# and Toshio Yanagida*#¶

*Department of Biophysical Engineering, Faculty of Engineering Science, Osaka University, Toyonaka, Osaka; #Biomotron Project, ERATO, (JST), Mino, Osaka; §Department of Applied Physics, School of Engineering, Nagoya University, Nagoya, Aichi; and ¶Department of Physiology, Osaka University Medical School, Suita, Osaka, Japan

ABSTRACT Displacements of single one-headed myosin molecules in a sparse myosin-rod cofilament were measured from bead displacements at various angles relative to an actin filament by dual optical trapping nanometry. The sparse myosin-rod cofilaments, 5–8 μm long, were synthesized by slowly mixing one-headed myosin prepared by papain digestion with myosin rods at molar ratios of 1:400 to 1:1500, so that one to four one-headed myosin molecules were on average scattered along the cofilament. The bead displacement was ~10 nm at low loads (~0.5 pN) and at angles of 5–10° between the actin and myosin filaments (near physiologically correct orientation). The bead displacement decreased with an increase in the angle. The bead displacement at nearly 90° was ~0 nm. When the angle was increased to ~150°-170°, the bead displacements increased to 5 nm. A native two-headed myosin showed similar size and orientation dependence of bead displacements as a one-headed myosin.

INTRODUCTION

Techniques for imaging a single actin filament (Yanagida et al., 1984) and manipulation of protein molecules by a microneedle (Kishino and Yanagida, 1988; Ishijima et al., 1991) and an optical trap (Svoboda et al., 1993; Svoboda and Block, 1994) have allowed forces and displacements to be measured directly from single myosin molecules bound to the surface of an artificial substrate (Finer et al., 1994, 1995; Ishijima et al., 1994, 1996; Miyata et al., 1994; Molloy et al., 1995a, 1995b; Guilford et al., 1997; Mehta et al., 1997). Finer and co-workers have measured the displacements of single myosin fragments, heavy meromyosin (HMM) randomly bound to the surface of a silica bead with dual optical trapping nanometry, and showed a displacement of ~10 nm (Finer et al., 1994, 1995). Molloy and colleagues have argued that to estimate the displacement of myosin from bead displacements, the randomizing effect of the thermal fluctuations of beads in optical traps or on a needle should be taken into account. Furthermore, the displacement produced by a two-headed myosin or its fragment may be different from that of a myosin head. They have measured the displacements of single one-headed myosin subfragment (S-1) molecules by the same method as Finer and co-workers (Finer et al., 1994) and determined the displacement by taking the randomizing effects into account. The displacement of an S-1 molecule under these conditions was 4–6 nm (Molloy et al., 1995a). A similar value was also obtained for HMM (Miyata et al., 1994; Mehta et al., 1997), which is consistent with that expected from the structural studies of the myosin head (Wakabayashi et al., 1992; Rayment et al., 1993a,b; Fisher et al., 1995a,b; Smith et al., 1995; Whittaker et al., 1995; Jontes et al., 1995). However, these displacements were obtained from S-1 and HMM molecules randomly oriented on the artificial surface, so the displacement values may have been influenced by the random orientation of the myosin molecules. Furthermore, the S-1 molecules may have been damaged during the interaction with the surface of the artificial substrate.

In vitro motility assays have shown that the relative sliding velocity (Sellers and Kachar, 1990; Yamada et al., 1990; Yamada and Wakabayashi, 1993; West et al., 1996) and force produced by the myosin heads (Ishijima et al., 1991, 1994, 1996) when an actin filament moves toward the central barezone of a myosin filament are both much greater than when an actin filament moves away from the center. These results suggest that the displacement of a myosin head would be affected by the orientation of the head. The velocity of actin filaments propelled by S-1 molecules bound directly to a glass surface is severalfold smaller than that produced by HMM and intact myosin molecules (Toyoshima et al., 1987). Recently Iwane and colleagues have shown that S-1 can move actin as fast as intact myosin when S-1 molecules are specifically bound to glass surface at their tail ends (regulatory light chains) by a biotin-avidin system (Iwane et al., 1997). Therefore, the displacement produced by S-1 molecules directly bound to the surface may be altered during interaction with the artificial surface.

To avoid such possible effects, we have measured the displacements of single one-headed myosin molecules in a sparse myosin rod cofilament at various angles relative to the actin filament axis using dual optical trapping nanometry. The results showed that the bead displacement of single one-headed myosin molecules, after correcting for the randomizing effect of the thermal motions of the beads

Received for publication 18 December 1997 and in final form 4 June 1998.

Address reprint requests to Dr. Toshio Yanagida, Department of Physiology 1, Osaka University Medical School, 2-2 Yamadaoka, Suita, Osaka, 565-0871, Japan. Tel.: 81-6-879-3620; Fax: 81-6-879-3628; E-mail: yanagida@phys1.med.osaka-u.ac.jp.

0006-3495/98/10/1886/09 $2.00

(Molloy et al., 1995a), was ~10 nm at low loads (maximum force ~0.5 pN) and 5–10° (near physiologically correct orientation). The bead displacement averaged over all directions from ~0° to ~180° was calculated to be ~5 nm. This value is consistent with those previously reported for S-1 and HMM molecules randomly oriented on the surface (Molloy et al., 1995a; Mehta et al., 1997). Thus the small displacements previously reported are likely to be due to the effect of the random orientation of the myosin heads.

Furthermore, the displacement produced by a myosin head may be ~1.5-fold larger than the bead displacement, because the linkage between the actin filament and the bead and between the myosin molecule and the surface of a glass cannot be rigid, so that the bead displacement is attenuated by such compliance (Svoboda and Block, 1994; see Discussion).

MATERIALS AND METHODS

Protein preparation

All proteins were obtained from rabbit skeletal muscle. Myosin was extracted from muscle and purified (Harada et al., 1990). One-headed myosin was obtained by heavily digesting myosin with papain (Harada et al., 1987). Myosin rod was prepared and purified from myosin (Margossian and Lowey, 1982) and labeled with tetramethylrhodamine isothiocyanate (TRITC) (Molecular Probes, Eugene, OR) or fluorescein isothiocyanate (FITC) (Molecular Probes) as previously described (Ishijima et al., 1996). Myosin, one-headed myosin, rod, TRITC-labeled rod, and FITC-labeled rod were rapidly frozen in liquid nitrogen and stored at −80°C. G-actin was extracted from acetone powder and purified (Spudich and Watt, 1971). Actin filaments were labeled with phalloidin-tetramethylrhodamine isothiocyanate (PHD-TRITC) (Molecular Probes) as previously described (Harada et al., 1990).

Native polyacrylamide gel electrophoresis

The purity of the one-headed myosin preparation was checked by 3% polyacrylamide gel electrophoresis (PAGE) in the presence of 20 mM inorganic pyrophosphate according to the method of Harada and colleagues (Harada et al., 1987). The fractions of one-headed myosin and rod were estimated by densitometry (Spectrophotometer DU640; Beckman) of Coomassie blue-stained polyacrylamide gels.

Electron microscopy

The sample containing one-headed myosin and myosin rods on a mica film was examined by electron microscopy (JEM-1200EX; JEOL). The sample was rotary-shadowed using platinum (Harada et al., 1990). Native myosin molecules were observed as a control.

Synthesis of fluorescently labeled cofilaments of one-headed myosin and rod

One-headed or two-headed myosin, rod, and TRITC-labeled rod were mixed in a solution containing 0.6 M KCl, 5 mM $MgCl_2$, 10 mM HEPES (pH 7.0), and the mixture was dialyzed against a solution of 0.12 M KCl, 5 mM $MgCl_2$, 10 mM HEPES (pH 7.0) overnight at 0°C without stirring (Ishijima et al., 1996). The total concentration of the three kinds of proteins was set at 0.15 μM, and the molar ratio of one-headed myosin to rod in the mixture was adjusted from 1:400 to 1:1500, or two-headed myosin to rod from 1:800 to 1:3000, in which 1% TRITC-labeled rod was included. The number of myosin heads in a cofilament was determined by fluorescence images of individual Cy3ATP (or ADP) molecules bound to the myosin heads under a refined total internal reflection microscope (Funatsu et al., 1995). When the sliding movement of actin filaments along a myosin-rod cofilament was observed, filaments were synthesized by mixing one- or two-headed myosin and rod at a molar ratio of 1:5, in which 8% FITC-labeled rod was included. The sliding movement of actin filaments along a myosin-rod cofilament in vitro was observed by the same method as previously described (Ishijima et al., 1996).

NEM-treated, myosin-coated beads

Polystyrene fluorescent beads (diameter = 0.83 μm, Covaspheres Reagent MX Blue Fluorescing; Duke Scientific Co., Palo Alto, CA) were incubated with *N*-ethylmaleimide (NEM)-treated myosin (1 mg/ml) at 0°C for 60 min. NEM-treated, myosin-coated beads were washed by repeated centrifugation for 10 min at 15,000 rpm and resuspended in a buffer containing 25 mM KCl, 5 mM $MgCl_2$, 20 mM HEPES (pH 7.8).

Chemical etching of coverslips

In our experiments, myosin cofilaments had to be raised from the glass surface to a level higher than the bead radius. To achieve this, pedestals were made on the glass surface by chemically etching the coverslips (Fig. 1 *A*). Coverslips (24 mm × 32 mm; Matsunami Co., Osaka, Japan) were cleaned by washing in 0.1 M KOH and 100% ethanol. The clean surface was coated with chrome by vacuum evaporation and then coated with photoresist (AZ RFP210K; Hoechst, Sizuoka, Japan). Square patterns were printed on the surface by irradiating with a UV light through a square pattern mask (15 μm × 15 μm). The resist film was developed and the irradiated area was removed (AZ developer; Hoechst). The chrome unmasked with resist was removed with chrome etching solution (7.5 wt%

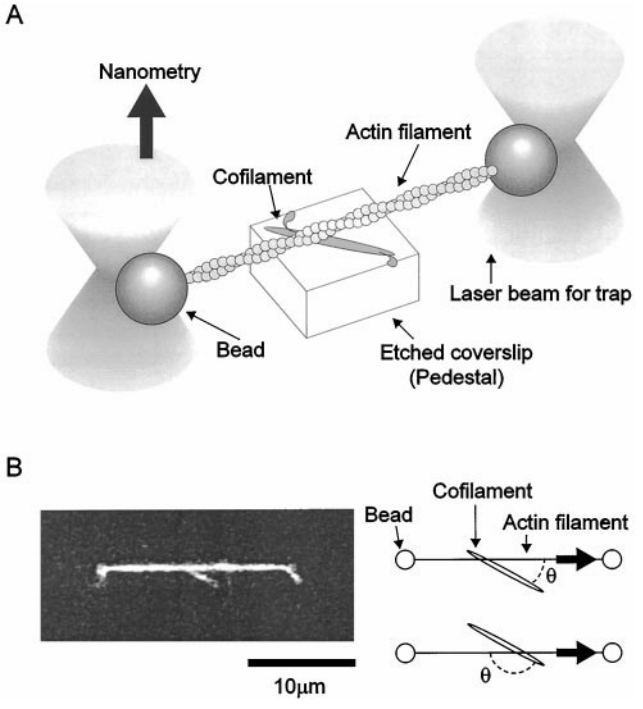

FIGURE 1 (*A*) Schematic diagram of the measurement system (see text for details). (*B*) An epifluorescence image of an actin filament interacting with a myosin-rod cofilament on the glass surface. A schematic drawing of this image is shown on the right. Thick arrows indicate the direction of force. θ is the angle between the actin filament and cofilament (see text).

$HClO_4$, 12.1 wt% $(NH_4)_2Ce(NO_3)_6$, 80.4 wt% H_2O), and then the bare surface of the coverslip was etched in a solution containing 3% NH_4F and 50% H_2SO_4 for 15 min. Etched coverslips were rinsed with water, and the remaining chrome on the surface was removed with a chrome etching solution. This produced pedestals ~5–10 μm × 5–10 μm in area and 5 μm in height on the surface. The distance between adjacent pedestals was ~50 μm.

Displacement measurements

A solution containing myosin cofilaments was applied to the surface of an etched coverslip that had previously been treated with silicone (Harada et al., 1990) and coated with bovine serum albumin (0.5 mg/ml BSA) (Ishijima et al., 1996). After 5 min, unbound cofilaments were washed out with an assay buffer (see below). Actin filaments labeled with PHD-TRITC were mixed with NEM-treated, myosin-coated beads and introduced to the coverslip in the assay buffer. Actin filaments, one- or two-headed myosin-rod cofilaments, and beads were visualized under an epifluorescence microscope. An actin filament, with both ends attached to separate beads captured by dual optical traps, was then brought into contact with a myosin-rod cofilament on the surface of a pedestal (Fig. 1, *A* and *B*). The displacement of one of the beads was determined with a quadrant photodetector with nanometer accuracy (Fig. 1 *A*). Displacements were measured in an assay buffer containing 25 mM KCl, 5 mM $MgCl_2$, 1 μM ATP, 20 mM HEPES (pH 7.6) at 20–25°C. To reduce photobleaching, an oxygen scavenger system (0.11 mg/ml glucose oxidase, 18 μg/ml catalase, 2.3 mg/ml glucose, and 0.5% 2-mercaptoethanol) was added (Harada et al., 1990).

Angles between myosin-rod cofilaments and actin filaments, and the polarity of myosin-rod cofilaments were measured from their fluorescence images (Fig. 1 *B*).

Optical system

An optical trapping system was built on an inverted epifluorescence microscope (TMD-300; Nikon). The infrared laser (1064 nm, 500 mW, 7910-Y4-106; Spectra-Physics Lasers) was split into two beams by an acoustooptic deflector (AOD) (LS110XY-1.06; Isomet) and incorporated into the microscope adapted for dual optical traps. A green laser (532 nm, 100 mW, 140-0532-100; Lightwave) was used to excite fluorescently labeled actin, myosin-rod cofilaments, and beads, and for illumination of a bead for nanometry. A 100× oil immersion objective lens (Plan-Neofluar, NA 1.3; Zeiss) was used to observe both epifluorescence images and optical trapping procedures. The fluorescent image was displayed on a TV monitor (PVM-122J; Sony), using a high-sensitivity SIT camera (C-2741; Hamamatsu-Photonics). The transmitted image of one of the trapped beads was projected onto a quadrant photodiode (S994–13; Hamamatsu-Photonics) through another 100× oil immersion objective lens (A100, NA 1.3; Olympus). The photodiode detector bandwidth was 34 kHz. The outputs from the quadrant photodiode were recorded by a digital data recorder (RD-120TE; TEAC) at a sampling rate of 24 kHz and analyzed with a signal processor (R9211A; Advantest) and a personal computer (FM-V; Fujitsu). Trap stiffness was determined by measuring the Brownian movement of the beads, as $K_t = k_BT/\langle x^2\rangle$, where K_t is the trap stiffness, k_B is Boltzman's constant, T is the absolute temperature of the fluid medium, and $\langle x^2\rangle$ is the variance of the Brownian movement of the trapped bead (Ishijima et al., 1996; Simmons et al., 1996; Guilford et al., 1997; Kojima et al., 1997).

RESULTS

Preparations of one-headed myosin and cofilaments

Fig. 2 *A* shows native PAGE patterns of myosin before (*left*) and after heavy digestion by papain (*right*) in the presence of 20 mM inorganic pyrophosphate (PP_i). The gels were stained with Coomassie blue. Densitometry of the patterns showed that the molar ratio of two-headed myosin, one-headed myosin, and rod after papain digestion was <0.01: 0.1–0.3:0.7–0.9, respectively. As contamination by two-headed myosin was too small to be detected by native PAGE, the numbers of two-headed and one-headed myosin molecules were counted by rotary-shadow electron microscopy. The electron micrographs of two-headed and one-headed myosin molecules are shown in Fig. 2 *B*. The ratio of two-headed and one-headed myosins was <0.02. Rods were not removed from the sample because very sparse one-headed myosin-rod cofilaments were used in experiments (see below).

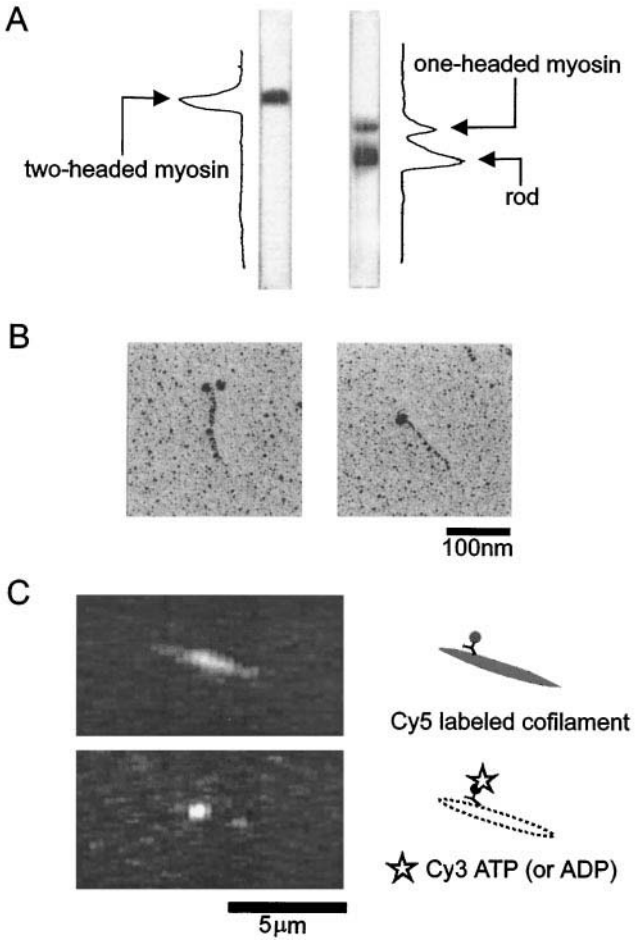

FIGURE 2 Preparation of one-headed myosin. (*A*) Three percent native PAGE patterns of native myosin (*left*) and one-headed myosin after papain digestion (*right*) in the presence of 20 mM PP_i. Solid lines show the densitometries of the gels stained with Coomassie blue. (*B*) Electron micrographs of a native myosin (*left*) and a one-headed myosin after papain digestion (*right*). (*C*) Fluorescence images of a myosin-rod cofilament labeled with Cy5 (*upper panel*) and Cy3-ATP or -ADP bound to the cofilament (*lower panel*). A schematic drawing of the image is shown on the right. The cofilament contains one myosin head.

Long filaments, 5–8 μm in length, were synthesized by slowly mixing one-headed myosin and rod in a molar ratio of 1:5 for motility measurements and 1:400–1500 for displacement measurements. The sliding velocity of single actin fila-

ments toward the center of a cofilament was approximately four times faster than that in the opposite direction. The sliding velocities and orientation dependence were both consistent with those for synthetic two-headed myosin filaments under the same conditions (Ishijima et al., 1996).

The number of one-headed myosin molecules in a cofilament was determined by observing fluorescence from bound Cy3-ATP/ADP molecules under a low background total internal reflection fluorescence microscope (Funatsu et al., 1995). The number of one-headed myosin molecules was one to four, as expected from the molar ratio of one-headed myosin and rod in the cofilament (Fig. 2 *C*).

Displacements of single one-headed myosin molecules

To measure displacements from single myosin heads, we have used one-headed myosin-rod cofilaments containing a very low ratio of one-headed myosin molecules; the molar ratio of one-headed myosin:rod ranged from 1:400 to 1:1500. An actin filament could be placed in contact with a myosin-rod cofilament at several different angles (Fig. 1, *A* and *B*). As only one to four myosin heads were distributed over a filament 5–8 μm in length and a suspended actin filament was not positioned exactly parallel to a cofilament, the number of myosin heads that could interact with a suspended actin filament at the same time would be one at most. Fig. 3 shows the typical time course for the generation of displacements (Fig. 3 *A*) and stiffness (Fig. 3 *B*) determined by measuring variances in the fluctuations of the bead (Molloy et al., 1995a; Kojima et al., 1997). The displacements occasionally showed negative values, most probably due to the randomizing effect of the thermal fluctuations of a bead (Molloy et al., 1995a). Thus it was difficult to distinguish between the displacement spikes and the thermal fluctuations in the traces showing the generation of displacements. Therefore, the displacements have only been scored when the stiffness increased for longer than 0.1 s (Fig. 3 *B*), because, when the myosin head bound to the actin filament attached to the bead, the total stiffness of the system (including the trapped bead and the actomyosin bond) increased, hence reducing the Brownian motion of the bead. The period of 0.1 s is the shortest time necessary to identify the changes in the variance of Brownian motion of the bead. Therefore, displacements with durations shorter than 0.1 s have not been included in the analysis. In the presence of low concentrations of ATP, the myosin head generates force and then forms a rigor complex with actin for a considerable period of time before the head binds a new ATP molecule. This means that the duration of displacements is due to the formation of long-life rigor complexes. Therefore, the size of the displacements should be independent of their duration. Thus the scoring of displacements would not be biased by omitting durations less than 0.1 s. Fig. 4 shows histograms of the displacements of beads (*left column*) and durations of displacements (*right column*) at 6.7 ± 1.5° (*A*), 20 ± 4° (*B*), and 27 ± 1° (*C*) (mean ± SD), respectively. Five to seven different cofilaments were used to obtain data for each angle. Thirty to one hundred displacement spikes were counted for each experiment (each cofilament). Thus the histogram for each angle was constructed from 400–500 displacement spikes. The histograms include the displacements for all cofilaments at each angle. The bead displacements were widely distributed from −20 to +50 nm. The thermal fluctuations of beads could be well fitted with Gaussian distributions when no myosin heads interacted with the actin filament (*solid line*). This result is consistent with the interpretation that the large distribution is due mostly to the randomizing effect of the thermal fluctuations of the beads (Molloy et al., 1995a). According to this interpretation, the bead displacements caused by myosin heads are determined by the values at the centers of the distributions. The centers of the histograms, which include all displacement data at each angle (Fig. 4, *left column*), have been determined by performing least-squares fits to the histograms. These values are 10 ± 1, 6.5 ± 0.9, and 4.4 ± 0.9 nm at the angles 6.7 ± 1.5°, 20 ± 4°, and 27 ± 1°, respectively.

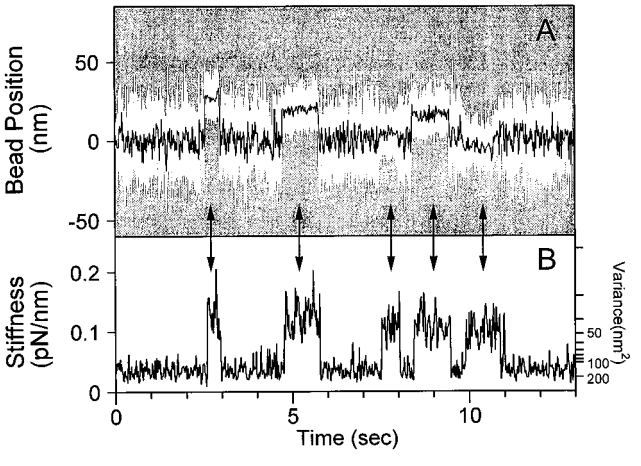

FIGURE 3 (*A*) Time course of the generation of displacements by a single one-headed myosin molecule at low load. White line, raw data. Black line, same data passed through a low-pass filter of 20 Hz bandwidth. (*B*) Changes in stiffness. The stiffness was obtained from the variance in the fluctuations of a bead. Displacements were scored when the stiffness increased, as shown by arrows (see text). The concentration of ATP was 1 μM, and the trap stiffness was 0.03 pN/nm. Temperature, 20°C.

The durations of displacements are shown in the right column of Fig. 4, where actin filaments interacted with cofilaments at angles of 6.7 ± 1.5° (*A*), 20 ± 4° (*B*), and 27 ± 1° (*C*), respectively. The histograms have been fitted with single exponentials by least-squares fits. The time constants were 0.22 ± 0.01 (*A*), 0.26 ± 0.02 (*B*), and 0.27 ± 0.02 s, respectively. The durations of the displacements were all similar.

Orientation dependence of displacements

Fig. 5 shows the bead displacements obtained at various angles between an actin filament and a myosin-rod cofila-

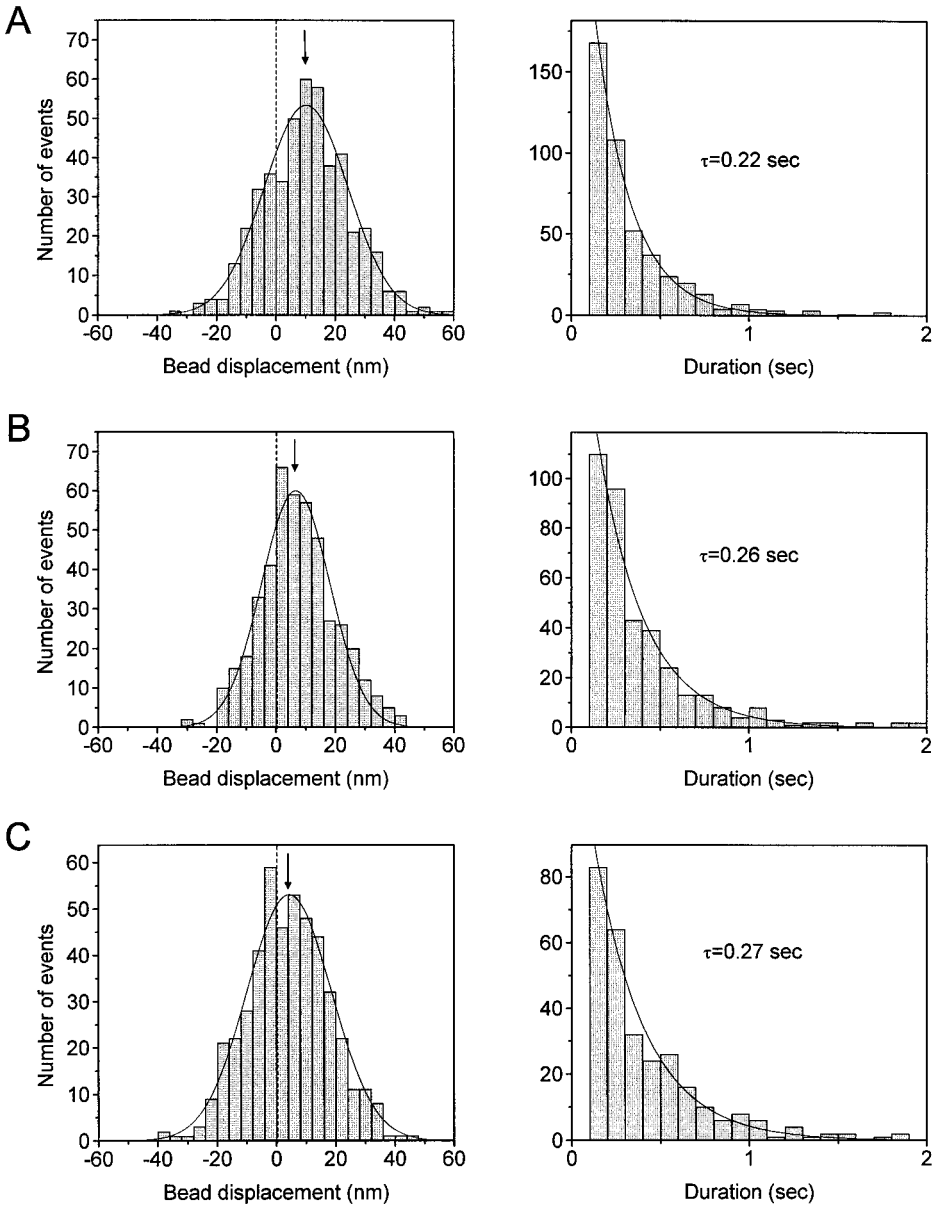

FIGURE 4 Histograms of bead displacements (*left column*) and durations of the displacements (*right column*) at angles between an actin filament and a cofilament of 6.7 ± 1.5° (*A*), 20 ± 4° (*B*), and 27 ± 1° (*C*) (mean ± SD). Five to seven different cofilaments were used to obtain data for each angle. The histograms include displacements for all cofilaments at each angle. (*Left column*) Solid lines show Gaussian distributions of the bead displacement, which have been determined by performing a least-squares fit to the histograms. The displacements of a bead are given by the shift of the Gaussian distribution from zero, and the values are 10 ± 1 (*A*), 6.5 ± 0.9 (*B*), and 4.4 ± 0.9 (*C*) nm, respectively. (*Right column*) Solid lines show single exponentials fitted to the distributions of displacement durations by least-squares fit. Time constants are shown in figures.

ment. Four to eight different cofilaments were used to obtain the data at each angle for one-headed myosin, and three to six different cofilaments at each angle for two-headed myosin. Twenty to one hundred displacement spikes were counted for each experiment (each cofilament). Thus the histogram for each angle was constructed from 100–500 displacement spikes. The centers of histograms were determined by least-squares fit to the histograms. The bead displacement was ~10 nm at 5–10° and decreased with an increase in the angle. At nearly 90°, no displacement spikes were observed despite the use of a myosin-rich cofilament. Interestingly, when the angle was increased further, the bead displacement increased with the angle and was ~5 nm at ~170°. Here, the angle and the direction of displacements were defined as follows. When the major direction of bead displacements was toward the center of a cofilament (forward direction), the acute angles between actin filaments and cofilaments were measured, and the displacements were defined as positive. When the major orientation was the away from the central bare zone (backward direction), the obtuse angles were measured and the displacements were defined as negative (refer to Fig. 1 *B*). Myosin-rod cofilaments, 5–8 μm long, were long enough to distinguish between the forward and backward regions of a cofilament observed under a fluorescence microscope.

Displacements of single two-headed myosin molecule

The displacements of two-headed myosin molecules were measured by a similar method. Fig. 6 *A* shows the typical

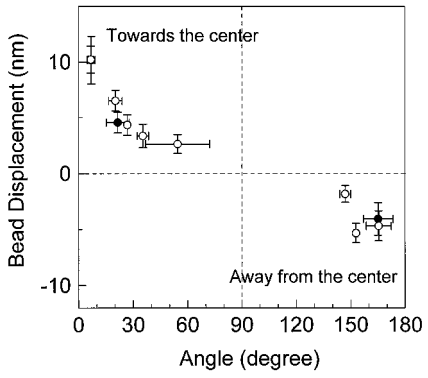

FIGURE 5 Orientation dependence of the displacements. Open and closed circles indicate displacements of one- and two-headed myosins, respectively. The displacement has been defined as positive when the displacement was toward the center of a cofilament (the sign of the displacement refers to the polarity of the myosin filament). See text for the definition of the angle and the sign of the displacements in detail. For each point, the error bars indicate the uncertainty of the mean bead displacement (*vertical axis*) and SD of the angle (*horizontal axis*). Four to eight different cofilaments were used to obtain the data at each angle for one-headed myosin, and three to six different cofilaments were used at each angle for two-headed myosin. Twenty to one hundred displacement spikes were counted for each experiment (each cofilament). Thus the histogram for each angle was constructed from 100–500 displacement spikes. The centers of histograms were determined by least-squares fit to the histograms.

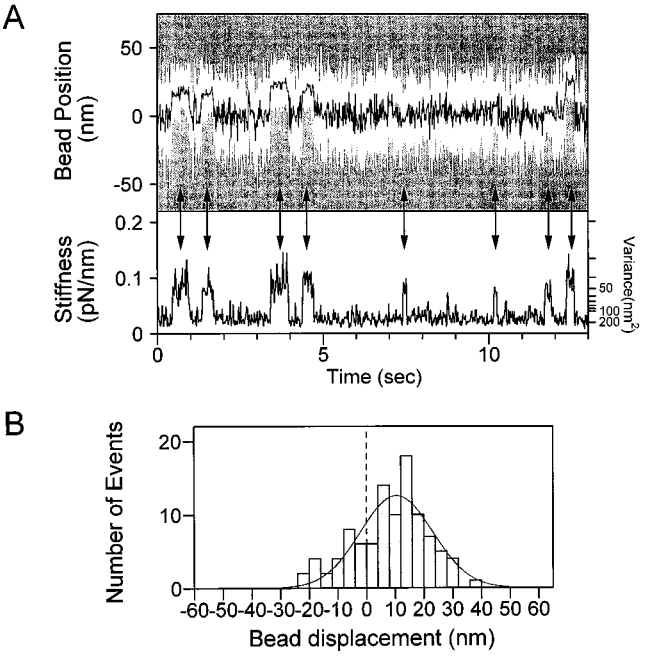

FIGURE 6 (*A*) Time course of the generation of displacements by a single two-headed myosin molecule at low load (*upper trace*; *white line*, raw data; the *black line* is the same data processed with a low-pass filter of 20 Hz bandwidth). The changes in the stiffness are shown in the lower trace. The stiffness was obtained from the variance of the fluctuations of a bead. Arrows indicate the interactions of actomyosin. The concentration of ATP was 1 μM, and the trap stiffness was 0.03 pN/nm. Temperature, 20°C. (*B*) Histogram of the bead displacements caused by a two-headed myosin molecule at an angle between an actin filament and cofilament of 6.9 $\pm$ 2.1° (mean $\pm$ SD). Three different cofilaments were used to obtain data. The histogram includes the displacements for all cofilaments at this angle. The solid line shows the Gaussian distributions of the bead displacement, which were determined by performing a least-squares fit to the histograms. The displacement of a bead is given by the shift of the Gaussian distribution from zero, and the value is 10 $\pm$ 2 nm.

time courses for the generation of displacements (*upper trace*) and the change in stiffness (*lower trace*) at an angle of 6.9 $\pm$ 2.1° between an actin filament and a cofilament. Fig. 6 *B* shows a histogram of the bead displacements. Three different cofilaments were used to obtain data. Twenty to fifty displacement spikes were counted for each experiment (each cofilament). The histogram includes the displacements for all cofilaments at an angle of 6.9 $\pm$ 2.1°. The center of the histogram was determined to be 10 $\pm$ 2 nm by a least-squares fit to the histogram. The size of the displacements and the dependence on myosin head orientation were both similar to those obtained for one-headed myosin (Fig. 5, *closed circles*). Three to six different cofilaments were used in these experiments.

DISCUSSION

Orientation dependence of displacements

The myosin head could interact with the actin filament at any angle between the actin and myosin filaments. This is probably due to the joint between the head and backbone of the myosin filament, most likely S2, having enough flexibility to allow the heads to thermally rotate. The rotational flexibility was examined by observing the thermal rotational fluctuations of a short actin filament ~4 μm long attached to a myosin head in a cofilament. The actin filament attached to the head rotated by more than 180° (Tanaka et al., manuscript in preparation). This result is consistent with that obtained for a kinesin molecule (Hunt and Howard, 1993). During thermal rotational fluctuations, the actin filament spent long periods at angles close to 0°, 180°, and 360°, and passed through angles of 90° and 270°, relatively quickly. This observation suggests that the head or neck region of a myosin molecule has some interaction with the polar backbone of a cofilament, or alternatively, the joint between the head and backbone may be stable when the head rotates by 0° and 180° relative to the tail region (light meromyosin). The orientation dependence of the displacements did not correspond to cos θ (Fig. 5). This is probably because the displacement depends on the interaction between the myosin head and backbone of a cofilament, as mentioned above.

The present result that the displacement at 0° was similar to that at 180° appears inconsistent with the previous findings that the velocity of an actin filament along a myosin filament at 180° is several times smaller than that at 0° at a saturated ATP concentration (physiologically correct angle; Sellers and Kachar, 1990; Yamada et al., 1990; Yamada and Wakabayashi, 1993; West et al., 1996; Ishijima et al., 1991, 1994, 1996). The sliding velocity, however, is determined not only by the size of the displacement, but also by the

detachment rate of the myosin head from actin after force generation. Therefore, the slower velocity at 180° would be due to a low detachment rate of the myosin head from actin. The sliding velocity of actin filaments on myosin filaments in vitro was measured at saturating ATP concentrations (>1 mM). At saturating ATP concentrations the attachment of ATP is not rate limiting, but rather ADP release (Siemankowski et al., 1985). In our experiments of step displacement, ATP attachment was rate limiting because of the very low ATP concentration (1 μM). It is not surprising, therefore, that our measurements of time constants do not vary with angle. Time constants at saturating ATP concentrations must be determined in separate experiments.

It is also possible that myosin molecules, which are accidentally oriented in a position that is the reverse of the rod alignment in a cofilament, could produce large displacements. This is unlikely, however, because displacements were observed at similar probabilities when an actin filament was brought into contact with cofilaments at 0° and 180°.

Size of displacements

Several investigators have previously reported, using dual optical trapping nanometry, that the displacements of single molecules of skeletal muscle myosin and its subfragments (S-1 and HMM) are 4–10 nm at low loads (Finer et al., 1994, 1995; Molloy et al., 1995a,b; Guilford et al., 1997; Mehta et al., 1997). Molloy and colleagues (Molloy et al., 1995a) have claimed that the displacements caused by a myosin head would be randomized by the thermal fluctuations of the beads, and thus the displacement should be corrected for this randomizing effect. The displacements of S-1 (Molloy et al., 1995a,b) and HMM (Mehta et al., 1997) after this randomizing correction are 4–6 nm. However, our present value of ~10 nm, which was measured as close to the correct orientation relative to the actin filament axis as possible and corrected for the randomizing effect, is significantly larger than these values. The previous experiments measured the displacements caused by single myosin fragments that were bound randomly to the artificial surface. Furthermore, the number of myosin heads that could interact with an actin filament was unknown, although low concentrations of fragments had been applied to the surface (1–2 μg/ml; Molloy et al., 1995b). Therefore, although each displacement spike was caused by a single myosin fragment, not all spikes observed in each experiment would have been produced by the same fragment. It is likely that the displacements were caused by many myosin fragments, all with different orientations. If this is correct, the displacements obtained in the previous experiments would be the values averaged over all orientations. The value averaged over all orientations in our experiments (Fig. 5) is ~5 nm, similar to the value previously obtained. Thus the smaller displacements obtained by the previous studies may be due to the effect of the random orientation of the myosin heads. Furthermore, it is also possible that the myosin heads may be affected by the interaction with the surface of an artificial substrate, especially when there is a low density of myosin heads on the surface, because myosin subfragments were directly bound to the surface in these previous studies.

In this study, we measured the bead displacements caused by a single myosin head. However, the bead displacements are usually smaller than the displacements caused by a myosin head (head displacement) because the head displacement is attenuated by the system compliance (Svoboda and Block, 1994). The head displacement can be obtained from the bead displacement as

$$D_{\text{head}} = D_{\text{bead}} \times (K_t + K_b)/K_b,$$

where D_{head} and D_{bead} are the displacements of a myosin head and a bead, respectively, K_t is the stiffness of the optical traps, and K_b is the total stiffness of the bonds between the beads and the actin filament and between the actin and myosin. If K_b is as large as that of an actomyosin cross-bridge (0.5–2 pN/nm; Huxley and Tideswell, 1996), $D_{\text{head}} \approx D_{\text{bead}}$, and no correction is necessary. K_t was determined by measuring the thermal fluctuations of the beads in each experiment (see Materials and Methods), and K_b was determined from the variance of the thermal fluctuations of a bead during the generation of a displacement for each displacement spike (Fig. 3 *A*). The average K_t and K_b in our present results are 0.03 and 0.06 pN/nm, respectively. The small stiffness of the system is probably due to components other than the actomyosin cross-bridge. Recently, Dupuis and co-workers (Dupuis et al., 1997) have reported that the system compliance is predominantly due to the flexibility of the actin filament near the filament-bead attachment. The average bead displacement near the physiologically correct orientation is 10 nm, so the head displacement can be calculated as 10 nm $\times$ (0.03 + 0.06)/0.06 = 15 nm.

To investigate the actual displacement of the myosin head and avoiding corrections, the stiffness of the measurement system (K_b) must be much higher than the trap stiffness (K_t). For example, an actin bundle would be useful for increasing the stiffness, because the actin bundle is stiff against both tension and compressive load (Kitamura et al., 1997).

One- and two-headed myosin

The size of displacements caused by a one-headed myosin molecule and the dependence on myosin head orientation could not be distinguished from those observations of a two-headed myosin molecule (Fig. 5). These results strongly suggest that the two heads of a myosin molecule do not interact with actin either simultaneously or sequentially. Recently, Katayama reported, using electron microscopy, that only one of the two heads of HMM interacted with an actin filament during sliding on HMMs bound to a mica surface (Katayama, 1998). This observation is consistent with our present results. In these in vitro motility assays,

however, a myosin molecule interacts with a single actin filament, so the two heads of a myosin molecule may not be interacting with the same actin filaments at the same time. In muscle, the two heads could interact with different actin filaments, so they would be able to generate force simultaneously or sequentially.

Our preparation of one-headed myosin was not 100% pure, but contained a small amount of two-headed myosin (2% of that of one-headed myosins). The average number of two-headed myosin molecules contained in one-headed myosin-rod cofilaments with the molar ratios used in our experiments (one-headed myosin:rod = 1:400–1:1500) is 0.08–0.03 per filament. Therefore, the possibility that the displacements observed in this study were caused by two-headed myosins would be very small. In these experiments, the actomyosin interactions have been observed with similar probabilities in both one- and two-headed myosin cofilaments. Thus the number of displacements caused by two-headed myosin molecules contained in one-headed myosin-rod cofilaments would be negligibly small.

The contamination of two-headed myosins in a one-headed myosin-rod cofilament was also tested by observing short actin filaments attached to myosin heads in the rigor state. Actin filaments have been shown to remain attached to a two-headed myosin molecule for lifetimes longer than 1 min (Nishizaka et al., 1995) or for more than 5 min in the absence of a load (Tanaka et al., manuscript in preparation). In contrast, the lifetime of an actin filament attaching to a one-headed myosin was, on average, ~100 s. Thus, under these conditions it was easy to distinguish between one-headed and two-headed myosin molecules.

The number of myosin heads interacting with an actin filament

To measure displacements from single one-headed myosin molecules, we have used myosin-rod cofilaments in which myosin molecules were very sparsely distributed. The molar ratios of myosin:rod were between 1:400 and 1:1500. Even though the average number of one-headed myosin molecules contained in these cofilaments ranged between one and four, it is possible that some cofilaments contained a greater number of heads. Therefore, when the actin filament is brought into contact with such a cofilament, especially when the angle between the actin filament and cofilament is small, the actin filament may interact with more than one head at the same time. To test this possibility, we measured the durations of displacements at various angles (Fig. 4, *right column*). The average durations were independent of the angles, and the second order association constant of ATP for actomyosin complexes has been calculated from the average durations (0.22–0.27 s) in the presence of 1 μM ATP as $1/(0.22–0.27\ \text{s})/1\ \mu\text{M} = (4–5) \times 10^6\ \text{M}^{-1}\ \text{s}^{-1}$. This value is consistent with that obtained for suspensions of acto-S1 in solution ($2 \times 10^6\ \text{M}^{-1}\ \text{s}^{-1}$; Woledge et al., 1985). These results exclude the possibility that the observed displacements were been produced by more than one myosin head.

Energetics

The movement of myosin heads is fuelled by the chemical energy from ATP hydrolysis. The chemical energy from hydrolysis of an ATP molecule is ~100 pN nm/molecule (Bagshaw, 1982). In this study, the displacement was 10 nm at a low trap stiffness (0.02–0.04 pN/nm). As the maximum forces were 0.3 pN, the work done by a myosin head has been calculated as $1/2 \times (10\ \text{nm}) \times (0.3\ \text{pN}) = 1.5\ \text{pN nm}$. This value corresponds to 1.5% of the chemical energy derived from the hydrolysis of an ATP molecule. In muscle, the maximum efficiency is ~50% at a load ~30% of that during isometric conditions (Woledge et al., 1985). If the displacement and force are both constant, independent of the load, and the efficiency is 50%, the maximum force can be calculated as $2 \times (100\ \text{pN nm} \times 0.5)/10\ \text{nm} = 10\ \text{pN}$. If the displacement is 4–6 nm as previously reported (Molloy et al., 1995a; Mehta et al., 1997) and is that expected from structural studies (Wakabayashi et al., 1992; Rayment et al., 1993a,b; Fisher et al., 1995a,b; Smith et al., 1995; Whittaker et al., 1995; Jontes et al., 1995), the force should be ~20 pN. Such a large force, however, would be unlikely, considering that the unbinding force of single actomyosin rigor complexes is ~9 pN (Nishizaka et al. 1995). Furthermore, if the force produced is smaller than the maximum force and the displacement is smaller than that at low load at the maximum efficiency, i.e., at ~30% of the maximum load, the maximum force should be larger than 20 pN. The maximum force under isometric conditions at the single molecule level has not been measured, because the stiffness of the experimental system is not high enough to produce the isometric condition.

We thank Dr. T. Funatsu and Dr. Y. Harada (ERATO) for their help in electron microscopy. We thank Dr. Nakayama and Dr. Oiwa (Kansai Advanced Research Center) for making the mask patterns used in the glass etching. We thank Dr. J. West (Monash University) for critically reading the manuscript and for valuable discussions.

REFERENCES

Bagshaw, C. R. 1982. Muscle Contraction. Chapman and Hall, London.

Burton, K. 1992. Myosin step size: estimates from motility assays and shortening muscle. *J. Muscle Res. Cell Motil.* 13:590–607.

Dupuis, D. E., W. H. Guilford, J. Wu, and D. M. Warshaw. 1997. Actin filament mechanics in the laser trap. *J. Muscle Res. Cell Motil.* 18: 17–30.

Finer, J. T., A. D. Mehta, and J. A. Spudich. 1995. Characterization of single actin-myosin interactions. *Biophys. J.* 68:291s–297s.

Finer, J. T., R. M. Simmons, and J. A. Spudich. 1994. Single myosin molecule mechanics: piconewton forces and nanometre steps. *Nature.* 368:113–119.

Fisher, A. J., C. A. Smith, J. Thoden, R. Smith, K. Sutoh, H. M. Holden, and I. Rayment. 1995a. Structural studies of myosin: nucleotide complexes: a revised model for the molecular basis of muscle contraction. *Biophys. J.* 68:19s–28s.

Fisher, A. J., C. A. Smith, J. B. Thoden, R. Smith, K. Sutoh, H. M. Holden, and I. Rayment. 1995b. X-ray structures of the myosin motor domain of *Dictyostelium discoideum* complexed with MgADP-BeFx and MgADP-AlF_4^-. *Biochemistry.* 34:8960–8972.

Funatsu, T., Y. Harada, M. Tokunaga, K. Saito, and T. Yanagida. 1995. Imaging of single fluorescent molecules and individual ATP turnovers by single myosin molecules in aqueous solution. *Nature.* 374:555–559.

Guilford, W. H., D. E. Dupuis, G. Kennedy, J. Wu, J. B. Patlak, and D. M. Warshaw. 1997. Smooth muscle and skeletal muscle myosins produce similar unitary forces and displacements in the laser trap. *Biophys. J.* 72:1006–1021.

Harada, Y., A. Noguchi, A. Kishino, and T. Yanagida. 1987. Sliding movement of single actin filaments on one-headed myosin filaments. *Nature.* 326:805–808.

Harada, Y., K. Sakurada, T. Aoki, D. D. Thomas, and T. Yanagida. 1990. Mechanochemical coupling in actomyosin energy transduction studied by in vitro movement assay. *J. Mol. Biol.* 216:49–68.

Hunt, A. J., and J. Howard. 1993. Kinesin swivels to permit microtubule movement in any direction. *Proc. Natl. Acad. Sci. USA.* 90: 11653–11657.

Huxley, A. F., and S. Tideswell. 1996. Filament compliance and tension transients in muscle. *J. Muscle Res. Cell Motil.* 17:507–511.

Ishijima, A., T. Doi, K. Sakurada, and T. Yanagida. 1991. Sub-piconewton force fluctuations of actomyosin in vitro. *Nature.* 352:301–306.

Ishijima, A., Y. Harada, H. Kojima, T. Funatsu, H. Higuchi, and T. Yanagida. 1994. Single-molecule analysis of the actomyosin motor using nano-manipulation. *Biochem. Biophys. Res. Commun.* 199: 1057–1063.

Ishijima, A., H. Kojima, H. Higuchi, Y. Harada, T. Funatsu, and T. Yanagida. 1996. Multiple- and single-molecule analysis of the actomyosin motor by nanometer-piconewton manipulation with a microneedle: unitary steps and force. *Biophys. J.* 70:383–400.

Iwane, A. H., K. Kitamura, M. Tokunaga, and T. Yanagida. 1997. Myosin subfragment-1 is fully equipped with factors essential for motor function. *Biochem. Biophys. Res. Commun.* 230:76–80.

Jontes, J. D., E. M. Wilson-Kubalek, and R. A. Milligan. 1995. A 32° tail swing in brush border myosin I on ADP release. *Nature.* 378:751–753.

Katayama, E. 1998. Quick-freeze deep-etch electron microscopy of the actin-heavy meromyosin complex during the in vitro motility assay. *J. Mol. Biol.* 278:349–367.

Kishino, A., and T. Yanagida. 1988. Force measurements by micromanipulation of a single actin filament by glass needles. *Nature.* 334:74–76.

Kitamura, K., M. Tokunaga, A. Iwane, K. Saito, and T. Yanagida. 1997. Manipulation and nanometer measurement of a single motor protein molecule captured directly by a scanning probe. *Biophys. J.* 72(Part 2):A55.

Kojima, H., E. Muto, H. Higuchi, and T. Yanagida. 1997. Mechanics of single kinesin molecules measured by optical trapping nanometry. *Biophys. J.* 73:2012–2022.

Margossian, S. S., and S. Lowey. 1982. Preparation of myosin and its subfragments from rabbit skeletal muscle. *Methods Enzymol.* 85:55–71.

Mehta, A. D., J. T. Finer, and J. A. Spudich. 1997. Detection of single-molecule interactions using correlated thermal diffusion. *Proc. Natl. Acad. Sci. USA.* 94:7927–7931.

Miyata, H., H. Hakozaki, H. Yoshikawa, N. Suzuki, K. Kinosita, Jr., T. Nishizaka, and S. Ishiwata. 1994. Stepwise motion of an actin filament over a small number of heavy meromyosin molecules is revealed in an in vitro motility assay. *J. Biochem.* 115:644–647.

Molloy, J. E., J. E. Burns, J. Kendrick-Jones, R. T. Tregear, and D. C. S. White. 1995a. Movement and force produced by a single myosin head. *Nature.* 378:209–212.

Molloy, J. E., J. E. Burns, J. C. Sparrow, R. T. Tregear, J. Kendrick-Jones, and D. C. S. White. 1995b. Single-molecule mechanics of heavy meromyosin and S1 interacting with rabbit or *Drosophila* actins using optical tweezers. *Biophys. J.* 68:298s–305s.

Nishizaka, T., H. Miyata, H. Yoshikawa, S. Ishiwata, and K. Kinosita, Jr. 1995. Unbinding force of a single motor molecule of muscle measured using optical tweezers. *Nature.* 377:251–254.

Rayment, I., H. M. Holden, M. Whittaker, C. B. Yohn, M. Lorenz, K. C. Holmes, and R. A. Milligan. 1993a. Structure of the actin-myosin complex and its implications for muscle contraction. *Science.* 261: 58–65.

Rayment, I., W. R. Rypniewski, K. Schmidt-Bäse, R. Smith, D. R. Tomchick, M. M. Benning, D. A. Winkelmann, G. Wesenberg, and H. M. Holden, 1993b. Three-dimensional structure of myosin subfragment-1: a molecular motor. *Science.* 261:50–58.

Sellers, J. R., and B. Kachar. 1990. Polarity and velocity of sliding filaments: control of direction by actin and of speed by myosin. *Science.* 249:406–408.

Siemankowski, R. F., M. O. Wiseman, and H. D. White. 1985. ADP dissociation from actomyosin subfragment 1 is sufficiently slow to limit the unloaded shortening velocity in vertebrate muscle. *Proc. Natl. Acad. Sci. USA.* 82:658–662.

Simmons, R. M., J. T. Finer, S. Chu, and J. A. Spudich. 1996. Quantitative measurements of force and displacement using an optical trap. *Biophys. J.* 70:1813–1822.

Smith, C. A., and I. Rayment. 1995. X-ray structure of the magnesium(II)-pyrophosphate complex of the truncated head of *Dictyostelium discoideum* myosin to 2.7 Å resolution. *Biochemistry.* 34:8973–8981.

Spudich, J. A., and S. Watt. 1971. The regulation of rabbit skeletal muscle contraction. I. Biochemical studies of the interaction of the tropomyosin-troponin complex with actin and the proteolytic fragments of myosin. *J. Biol. Chem.* 246:4866–4871.

Svoboda, K., and S. M. Block. 1994. Force and velocities measured for single kinesin molecules. *Cell.* 77:773–784.

Svoboda, K., C. F. Schmidt, B. J. Schnapp, and S. M. Block. 1993. Direct observation of kinesin stepping by optical trapping interferometry. *Nature.* 365:721–727.

Toyoshima, Y. Y., S. J. Kron, E. M. McNally, K. R. Niebling, C. Toyoshima, and J. A. Spudich. 1987. Myosin subfragment-1 is sufficient to move actin filaments in vitro. *Nature.* 328:536–539.

Wakabayashi, K., M. Tokunaga, I. Kohno, Y. Sugimoto, T. Hamanaka, Y. Takezawa, T. Wakabayashi, and Y. Amemiya. 1992. Small-angle synchrotron x-ray scattering reveals distinct shape changes of the myosin head during hydrolysis of ATP. *Science.* 258:443–447.

West, J. M., H. Higuchi, A. Ishijima, and T. Yanagida. 1996. Modification of the bi-directional sliding movement of actin filaments along native thick filaments isolated from a clam. *J. Muscle Res. Cell Motil.* 17: 637–646.

Whittaker, M., E. M. Wilson-Kubalek, J. E. Smith, L. Faust, R. A. Milligan, and H. L. Sweeney. 1995. A 35-Å movement of smooth muscle myosin on ADP release. *Nature.* 378:748–751.

Woledge, R. C., N. A. Curtin, and E. Homsher. 1985. Energetic Aspects of Muscle Contraction. Academic Press, London.

Yamada, A., N. Ishii, and K. Takahashi. 1990. Direction and speed of actin filaments moving along thick filaments isolated from molluscan smooth muscle. *J. Biochem.* 108:341–343.

Yamada, A., and T. Wakabayashi. 1993. Movement of actin away from the center of reconstituted rabbit myosin filament is slower than in the opposite direction. *Biophys. J.* 64:565–569.

Yanagida, T., M. Nakase, K. Nishiyama, and F. Oosawa. 1984. Direct observation of motion of single F-actin filaments in the presence of myosin. *Nature.* 307:58–60.